

Oil–water flows through sudden contraction and expansion in a horizontal pipe – Phase distribution and pressure drop

T. Balakhrisna^a, S. Ghosh^a, G. Das^{a,*}, P.K. Das^b

^a Department of Chemical Engineering, Indian Institute of Technology Kharagpur, Kharagpur 721 302, India

^b Department of Mechanical Engineering, Indian Institute of Technology Kharagpur, Kharagpur 721 302, India

ARTICLE INFO

Article history:

Received 3 April 2009

Received in revised form 7 August 2009

Accepted 10 August 2009

Available online 11 September 2009

Keywords:

Liquid–liquid flow

Core annular flow

Sudden contraction

Sudden expansion

ABSTRACT

In this paper, change of flow patterns during the simultaneous flow of high viscous oil and water through the sudden contraction and expansion in a horizontal conduit has been studied. It is noted that these sudden changes in cross-section have a significant influence on the downstream phase distribution of lube oil–water flow. The observation suggests a simple technique to establish core flow as well as a way to prevent pipe wall fouling during the transportation of such oil. A number of interesting differences have been noted during low viscous oil–water flow through the same test rigs. While several types of core annular flow are observed for the former case, a wider variety of interfacial distribution characterizes kerolene–water systems. The pressure profiles during the simultaneous flow of lube oil and water through the sudden contraction and expansion are also studied and compared with low viscous oil–water flows. The pressure profiles are found to be independent of liquid viscosity and the loss coefficients are observed to be independent of flow patterns in both the cases.

© 2009 Elsevier Ltd. All rights reserved.

1. Introduction

The last decade has reported an increasing number of studies on oil–water flows through conduits of different dimensions and geometries. Several investigations, both experimental and theoretical, have reported the interfacial distribution and the hydrodynamics of flow (Brauner, 1991; Bai et al., 1992; Bannwart, 1998, 2001; Angeli and Hewitt, 2000; Rodriguez and Bannwart, 2006; Charles et al., 1961; Oliemans et al., 1987; Arney et al., 1993; Chakrabarti et al., 2005). The studies have primarily been motivated by the continuous depletion of on-shore oil fields and the importance of cross-country transportation. In addition, the exhaustion of light oil reserves has called for a worldwide interest in transportation of high viscous crude.

A major challenge in this field is the huge pumping power required and several measures have been suggested to reduce the pumping power. One of the attractive proposals is the water-lubricated transport of heavy oils. This comprises of injecting water into the flow passage in such a way that water wets the pipe wall and the oil core flows through the central region. As a result, wall friction arises due to the flow of water only through the pipe and the pumping power reduces drastically. Owing to its industrial importance, both experimental and theoretical studies have been reported on different aspects of core annular flow. These include

estimation of the stable range of flow (Hickox, 1971; Ooms et al., 1984; Preziosi et al., 1989; Bai et al., 1996; Joseph et al., 1997), pressure drop (Bai et al., 1992; Arney et al., 1993; Bannwart, 1998; Sotgia et al., 2008; Grassi et al., 2008), wettability characteristics of the pipe material (Arney et al., 1996; Santos et al., 2006; Silva et al., 2006), nozzle design (Parda and Bannwart, 2001) and restart procedure (Arney et al., 1996). Simultaneous efforts have also been made to understand the mechanism of core levitation from a fundamental point of view. Ooms and Poesio (2003) used the lubrication theory, which assumes lubrication force on the core to be counterbalanced by buoyancy for a ripple in the form of a snake wave. However, this was not possible for a bamboo wave. Ooms et al. (2007) showed that the balance between buoyancy force and hydrodynamic force on the core makes eccentric core annular flow possible in a horizontal pipeline.

A survey of the literature on oil–water flow reveals that the majority of the past studies are confined to horizontal and vertical pipes of uniform cross-section. Not much is known about liquid–liquid flow across expansion and contraction, although these are common occurrences in cross-country transportation. In fact, the past survey has revealed only a few works on gas–liquid flow through expansion and contraction. Geiger (1964) has reported pressure drop of steam–water flows through sudden contraction for three different area ratios (0.144, 0.213, 0.398). McGee (1966) has noted the pressure drop for sudden contraction and expansion for two test rigs using steam–water as the test fluids. Studies are also reported by Janssen (1966). Delhaye (1981) has developed an

* Corresponding author. Tel.: +91 3222 283952; fax: +91 3222 255303.

E-mail address: gargi@che.iitkgp.ernet.in (G. Das).

analytical model for pressure recovery in sudden expansion for two-phase flows. Wadle (1989) has proposed an empirical correlation for pressure recovery in sudden expansion based on the experiments performed with steam–water as well as air–water. The model assumes that pressure recovery is proportional to the dynamic pressure head defined in terms of superficial velocities. Schmidt and Friedel (1997) suggested a model for predicting pressure drop at a sudden contraction and verified it with experimental data for air–water. They noted that unlike single-phase flows, a vena contract is not observed for two-phase flow when mass flow quality lies between 1% and 97%. Guglielmini et al. (1997) have also reported pressure drop studies. Fossa and Guglielmini (2002) have reported the pressure drop and void fraction profiles across different orifices. Subsequently, Fossa et al. (2006) have performed experiments with air–water to determine the flow structure across an orifice contraction. Ahmed et al. (2007) have performed experiments on air–oil flow in sudden expansion and reported that both the upstream and downstream flow regimes were similar to the flow pattern map of Taitel and Dukler (1976) for horizontal flows. However, the flow in the developing region and the developing length are dependent on the upstream flow pattern and the area ratio. They proposed an analytical model for pressure recovery downstream of the expansion. It predicts experimental data within 30%. Subsequently, Ahmed et al. (2008) observed the changes in flow patterns during the simultaneous flow of air and oil through sudden expansion in test rigs of two different area ratios. They reported the area ratio as well as the upstream flow pattern to influence the phase redistribution and the developing length downstream of the expansion. Chen et al. (2009) have performed experiments with air–water flow through sudden contraction in small rectangular channels of four different area ratios. They observed elongated bubbles to be the dominant flow pattern for low gas flux and mass quality. They have proposed a modified homogenous model, which takes into account the effect of contraction area ratio, gas quality and Bond and Weber number to predict the pressure drop. The only study on oil–water flows has been reported by Hwang and Pal (1997). They have obtained the pressure profiles and loss coefficients during flow of low viscous oil–water emulsion across sudden expansion and contraction of different area ratios.

No information till date is available on the change in liquid–liquid flow patterns due to the presence of a contraction/expansion to the best of the authors' knowledge.

With these considerations, the present study attempts to understand the behavior of oil–water flow when it encounters a sudden change in cross-section. Extensive experiments have been performed for an expansion as well as a contraction in the horizontal flow passage. Both high viscous and low viscous oils have been used as test fluids to note the influence of physical properties on flow and pressure drop characteristics.

2. Experimental setup and procedure

A schematic of the experimental setup has been presented in Fig. 1a. It comprises of two test rigs T1 and T2. Both consist of acrylic resin tubes of diameter 0.0254 m and 0.012 m. The total length of each of them is 7 m. In case of T1, the larger tube (i.d. = 0.0254 m) is followed by the smaller one while T2 has the reverse arrangement (the narrow tube is placed prior to the larger one). The ratio of the cross-sectional areas of the smaller to the larger pipe has been selected as 0.25 for both the cases.

The test fluids used in the experiments are lubricating oil, kerosene and water. Their physical properties are listed in Table 1. They are pumped from their respective tanks [OT, KT, WT in Fig. 1a] to the test passage. Three-way valves V1, V2 and V3 direct the respective flow of kerosene, water and lubricating oil to either T1 or T2. A high head (784.8 kPa) gear pump (P3) is used for lubricating oil while centrifugal pumps (P1) and (P2) are used for kerosene and water. The maximum discharge flow rate and head of the gear pump are $1.3 \times 10^{-3} \text{ m}^3/\text{s}$ and 784.8 kPa and that of centrifugal pumps $1.3 \times 10^{-3} \text{ m}^3/\text{s}$ and 294.3 kPa. Lube oil is metered using Coriolis mass flow meter [M] ranging from 0 to $2.5 \times 10^{-3} \text{ m}^3/\text{s}$ with a least count of $2.5 \times 10^{-5} \text{ m}^3/\text{s}$. Pre-calibrated rotameters [KR1, KR2, WR1, WR2] are used for measuring the flow rates of kerosene and water. The rotameters range from 0 to $1.67 \times 10^{-4} \text{ m}^3/\text{s}$ with a least count of $1.67 \times 10^{-6} \text{ m}^3/\text{s}$ and from 0 to $1.0 \times 10^{-3} \text{ m}^3/\text{s}$ with a least count of $3.33 \times 10^{-5} \text{ m}^3/\text{s}$ both for kerosene and water. The accuracy of flow rate measurement using the mass flow meter lies within $\pm 0.5\%$ and that using rotameters lies within $\pm 2\%$. The experimental errors in measuring the superficial velocities have been estimated to be within $\pm 0.43\%$ for lube oil and $\pm 1.9\%$ for the other liquids. The oil and water are introduced at the entry section through a specially designed nozzle [N]. A pictorial view of the nozzle is shown in Fig. 1b. The oil enters through the central portion of the nozzle

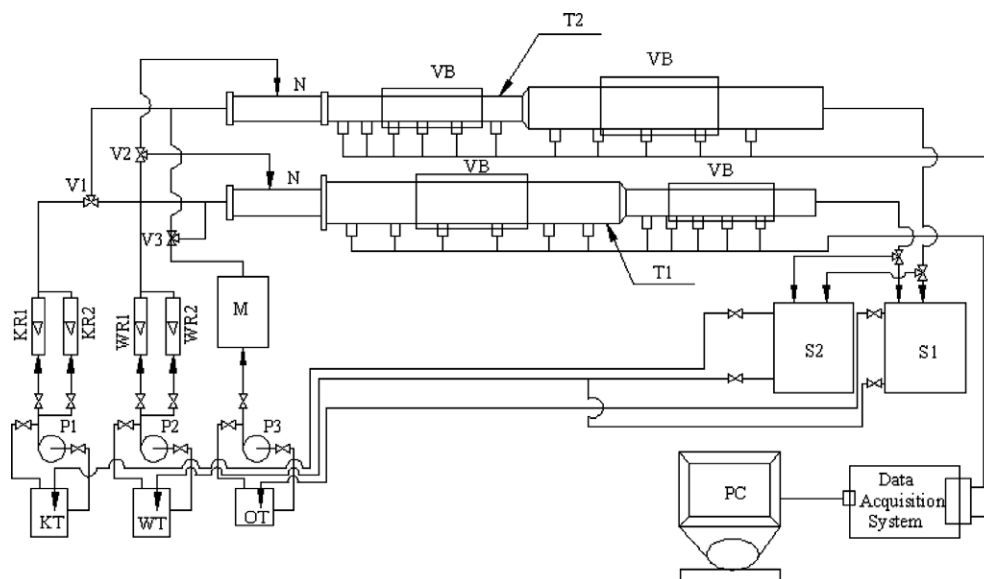


Fig. 1a. Schematic diagram of the experimental setup.

Table 1
Physical properties of the test fluids.

Fluid used	Density (kg/m ³)	Viscosity (Pa·s)	Surface tension (N/m)
Lubricating oil	960	0.2	0.039
Kerosene	787	0.0012	0.027
Water	1000	0.001	0.072

while water is injected in the annular space. From the test section, the two-phase mixture enters the separator (S1 for kerosene–water and S2 for lube oil–water). Here they are gravity separated and recycled back to their respective storage tanks.

The flow patterns for different combinations of oil and water velocities are observed visually and photographed by a high-speed digital camera (DSCH9, SONY). The view boxes (VBs) are used to minimize the optical distortion. Two schemes of changing the flow velocities have been adopted for test runs. Initially, oil velocity is increased at a constant water flow rate. The water velocity is then changed and the readings are repeated. Next, experiments are carried out at a constant oil velocity while water velocity is varied. This exercise is expected to detect the presence of hysteresis, if any. No significant difference in flow distribution has been noted for either of the two schemes of measurements.

The pressure profiles are noted by measuring the pressure drop at nine points with the first pressure tap at 1.0 m upstream of the plane of area change as the reference. The detailed arrangements of the pressure tapings are shown in Fig. 1a. Four pressure taps are located at distances of 0.03 m, 0.25 m, 0.5 m and 0.75 m upstream and five taps are located at 0.03 m, 0.25 m, 0.5 m and 0.75 m, and 1.0 m downstream from the contraction or expansion plane. Honeywell 24PCB differential pressure transducers have been used to measure the pressure drop. The transducer has a least count of 1.0×10^{-2} Pa and an accuracy of $\pm 2\%$ within the range of the experimental conditions studied.

3. Results and discussions

3.1. Flow patterns observed for lube oil–water flow

The various flow distributions of lube oil and water are depicted in Fig. 2. The range of existence of the aforementioned flow pat-

terns have been presented in the form of maps in Fig. 3. The superficial velocities of oil (U_{so}) and water (U_{sw}) are selected as the ordinate and abscissa of the maps. Fig. 3a and b represent the phenomena in the upstream and the downstream, respectively, of the contraction for test section T1. Similarly, Fig. 3c and d represents the flow patterns in the upstream and the downstream of the expansion in T2. The important flow patterns as observed from the figures are as follows

(a) Core annular regime: In both the test sections the flow phenomena mainly comprises of different types of core annular flow where, oil flows as a central core and water propagates as an annular film between the pipe wall and the oil core. Mainly three types of core flow have been observed – thick core, thin core and sinuous core.

Thick core flow is depicted by the representative photograph and schematic in Fig. 2a. The thick oil core is essentially eccentric with a thin water film at the top and a relatively thick film at the bottom surface of the tube. Further, the top surface of the core is smooth while its bottom part has a regular wavy pattern. The amplitude and wavelength of the structure depend on phase velocities. This distribution is observed in the larger tube for both the test rigs (Fig. 3a and d).

Thin core flow prevails in the narrow tube. It is noted at the downstream section of T1 over the entire range of oil velocities at low water flows (Fig. 3b) and the upstream section of T2 (Fig. 3c) beyond a particular oil velocity ($U_{so} > 0.5$ m/s). Fig. 2b reveals that the thin core has waviness and non-uniformity in the cross-section. The clearly visible water film at the wall also denotes the shift of the core to the central region of the pipe.

Sinuous core flow is a variation of thin core flow and can be distinguished from it by two interesting features. Firstly, the sinuous core has a wavy structure with a long wavelength and low amplitude. Secondly, oil droplets in large number are generated due to interfacial shear and are entrained in the water film (Fig. 2c). It occurs in test section T1 (Fig. 3a and b) at moderate velocities of the two liquids.

(b) Oil dispersed flow: This regime is observed at a very low oil flow rate and a relatively higher water velocity ($U_{sw} > 0.7$ m/s). As the name suggests, it is characterized by a dense dispersion of the oil phase in the continuous water medium. This gives the test rig a

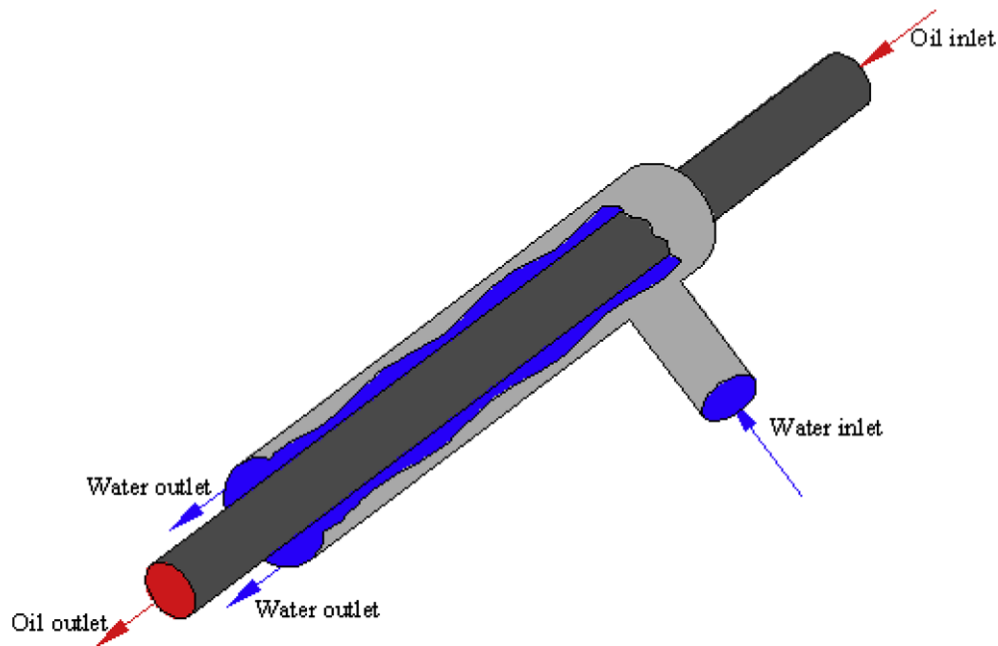


Fig. 1b. Schematic diagram of the nozzle.

Flow regimes	Schematic	Photographs
(a) Thick core flow		
(b) Thin core flow		
(c) Sinuous core		
(d) Oil dispersed flow		
(e) Plug flow		
(f) Distorted plugs		

Fig. 2. Representative photographs and schematics of lube oil–water flow regimes.

uniform yellowish¹ appearance. A representative photograph of the flow situation is depicted in Fig. 2d.

(c) Plug flow: This is characterized by alternate appearance of oil and water plugs in the flow passage. The water plugs are generally free from dispersed oil droplets and the oil plugs assume two different shapes in the present test sections. In the first case they are regular cylindrical in shape and are surrounded by a thin water film (Fig. 2e). In the latter case, they are thin and present a sinuous rope like structure (Fig. 2f). The distorted plugs are observed only in the narrow tube for both the test rigs at low oil and moderate water velocities.

3.1.1. The influence of sudden change in cross-sectional area on phase distribution

A comparative study of Fig. 3a–d reveals some interesting features.

- From Fig. 3a and b, it is noted that thick core flow gives way to thin core as it encounters a contraction in the flow passage. This indicates that the chances of pipe wall fouling can be minimized by directing the flow through a sudden contraction.
- A comparison of Fig. 3c and d reveals that all flow distributions get transformed to thick core flow as the two liquids encounter an expansion. This suggests that an effective way to establish core flow is to direct the two-phases across an expanded test section. It is interesting to note that several efforts in the past

have been directed to design a suitable nozzle for establishing core annular flow of high viscous oils to reduce its pumping power. The present study suggests that a simple entry comprising of an abrupt expansion can possibly ensure stable core flow in a pipeline although it does enhance the chances of pipe fouling.

- It may further be noted that while several past researchers working on the simultaneous flow of high viscous oil and water have reported a distribution similar to thick core flow, none of the studies have revealed thin core and sinuous core with entrained droplets to the best of the authors' knowledge.
- There are considerable differences in lube oil–water flow patterns in a horizontal pipe depending on the location of the pipe prior to or after the change in cross-section.
 - Fig. 3a indicates the existence of core annular, sinuous core, plug and dispersed flow in the 0.025 m diameter pipe while Fig. 3d depicts only core annular characteristics throughout the entire range of flow conditions when the same pipe is placed after an expansion.
 - In general, sinuous core is not observed in the narrow pipe (Fig. 3c) while it occupies a large area in the flow pattern map of Fig. 3b where the narrow pipe follows an abrupt contraction.
 - The range of existence of core annular and distorted plugs is also different in Fig. 3b and c.
 - An abrupt contraction brings about dispersed flow at high water and low oil velocities while it suppresses the formation of regular plugs, which can be noted in Fig. 3c but are absent in Fig. 3b.

¹ For interpretation of the references to color in Fig. 2, the reader is referred to the web version of this paper.

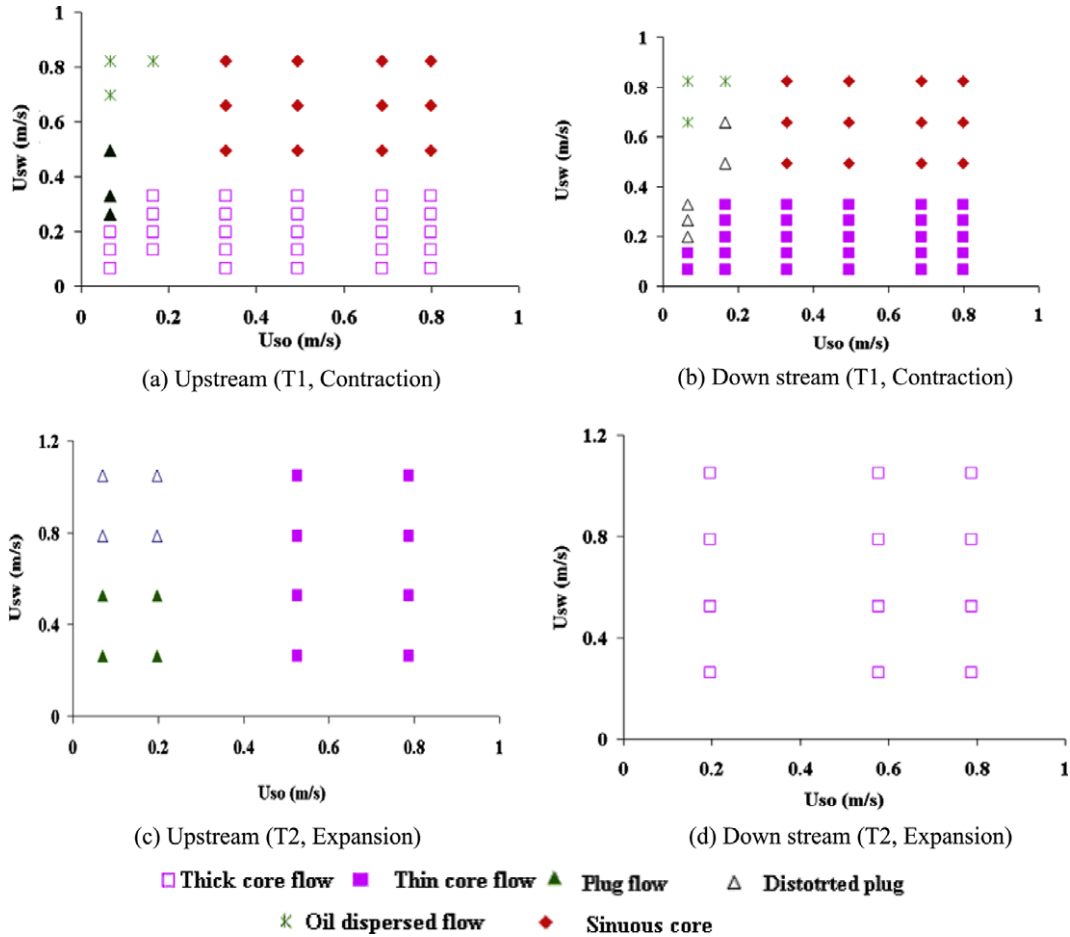


Fig. 3. Flow pattern maps for lube oil–water sudden contraction/expansion.

A few representative photographs depicting the influence of area change on flow distribution are shown in Figs. 4a and 4b. Fig. 4a clearly indicates the influence of contraction at lower water velocities and the similar phase distribution at high water flows. Fig. 4b depicts the thickening of the oil core as a lube oil–water mixture encounters an expanded passage.

3.2. A comparison with the flow patterns obtained for kerosene–water system

It could be interesting to note the differences in phase distribution when low viscosity oil and water are directed through the same test rigs under similar flow conditions. Fig. 5 depicts the schematic and representative photographs of various distributions during kerosene–water flow under the present range of experimental conditions. An optical probe is used as an additional check to the visualization and photographic studies. The details of the probe are given elsewhere (Jana et al. 2006). Fig. 5 shows that the distributions comprise of stratified flow, dispersed flow and an intermediate pattern between the two. The stratified configuration observed at low flow rates is characterized by a smooth interface. Interfacial waviness sets in with the increase in velocity of either of the fluids. The dispersion is oil-in-water at low oil and high water velocities and gets inverted to water-in-oil at high oil and low water flows. The transition between the two types of dispersion has been depicted as the ambivalent zone in the figure following the terminology by Chakrabarti (2006). The intermediate pattern is either plug at low oil or three layers at high oil velocities. A detailed description of the aforementioned patterns is provided by Chakrabarti (2006) in

a 0.0256 m diameter horizontal pipe and Mandal et al. (2007) in a 0.0127 m diameter tube. So to avoid repetition the details are not discussed in the present text and the range of existence of the flow regimes are presented as maps in Fig. 6a and b for T1 (contraction) and in Fig. 6c and d for T2 (expansion). A close observation of the figures provides the following noteworthy features:

- Almost similar distribution is observed at the upstream and downstream sections of a contraction (T1) and only slight differences are observed in the range of existence of the different patterns.
- On the other hand, an expansion (in T2) appears to influence the phase distribution to a greater extent particularly at low water velocities. The interfacial waves upstream of the expansion break down to form the three-layer pattern as it enters the wider tube of T2. The onset of dispersed flow is also observed at lower water velocities in the later cases.
- In general, the initiation of the different flow regimes takes place at lower phase velocities in Fig. 6b as compared to Fig. 6c. This can probably be attributed to the increased effect of turbulence at the abrupt contraction.
- Notable differences are also evident from a comparative study of Fig. 6a and d. This highlights the fact that flow patterns are not guided solely by fluid physical properties and conduit characteristics. There can be drastic errors if the exact conditions of flow are not accounted for.
- There are significant differences between lube oil–water flow and kerosene–water flow across an abrupt area change. While different variations of core annular flow mark the previous

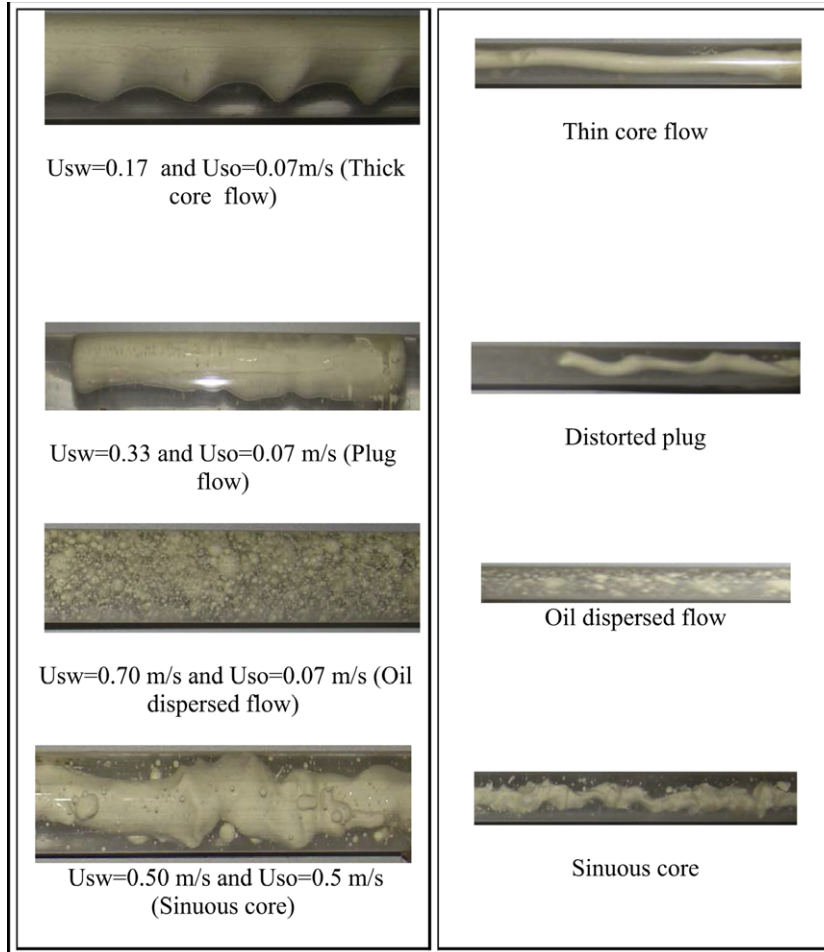


Fig. 4a. Photographs of flow patterns for lube oil–water in T1 (contraction).

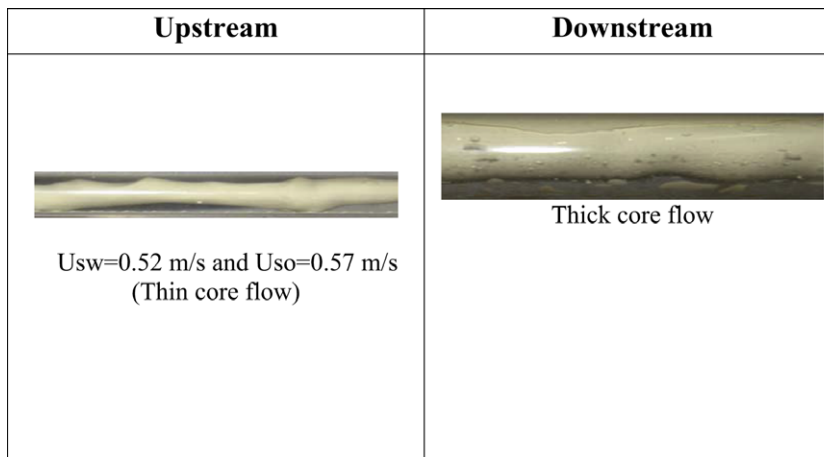


Fig. 4b. Photographs of flow patterns for $U_{so} = 0.57$ m/s in T2 (expansion).

situation, the distribution of kerosene–water ranges from completely separated to fully dispersed flow. However, core flow was never observed under the present range of experimental conditions. Further, an abrupt change in flow cross-section appears to influence lube oil–water flows to a greater extent as compared to kerosene–water flows.

3.3. Pressure profiles

Extensive measurements of pressure drop have been carried out over a wide range of superficial flow velocities ranging from 0.15 to 1 m/s for both the phases in order to understand the effect of area change and fluid viscosities on the pressure profiles. The pressure









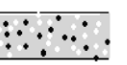

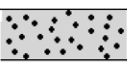



Flow regimes	Schematic	Photographs
(a) Stratified smooth		
(b) Stratified wavy		
(c) Plug flow		
(d) Three layers		
(e) Ambivalent		
(f) Oil in water dispersion		
(g) Water in oil dispersion		

Fig. 5. Representative photographs and schematics of kerosene–water flow regimes.

profiles are presented in Fig. 7a and b, respectively, for lube oil–water flow through contraction (T1) and expansion (T2). Fig. 8a and b depicts the same for kerosene–water flow. All the figures represent the absolute value of measured two-phase pressure drop (Δp_{ow}) as a function of tapping distance (denoted by \times in the figures) from the plane of area change. The figures show similar trend of pressure profiles for both the oils. Flow through T1, the pressure drop is almost uniform and independent of water velocity upstream of the contraction. From the point of contraction, it starts increasing along the length of the pipe due to high frictional losses and sudden area changes (Figs. 7a and 8a). This is similar to the trend obtained by Schmidt and Friedel (1997) for air–water flow through sudden contraction in a vertical rig.

Figs. 7b and 8b depict the pressure profiles of lube oil–water and kerosene–water in T2. In this case also, the trends of the profiles are similar for both the oils. The pressure drop increases along the length of the pipe up to the expansion point. It then falls to a slightly lower value for lube oil–water flow (Fig. 7b) and henceforth remains constant. Further, the trends of both the pressure profiles are in agreement with the reported results of Hwang and Pal (1997). However, for kerosene–water flow the pressure drop rises steeply at the plane of area change. A close observation of Figs. 7a and 8a further reveals that at T1, pressure drop in case of kerosene–water flow is higher than lube oil–water for the same superficial velocity of water. The reason behind this can be attributed to the existence of core annular flow in the former case. This highlights the advantage of core flow during transport of viscous oils to cross-countries and through sub sea pipelines. A reverse

trend is observed for flow through expansion. In this case the pressure drop of kerosene–water is slightly lower than lube oil–water for the same superficial velocity of water. This is evident from a comparison of Figs. 7b and 8b and can be attributed not only to the high oil viscosity but also to fouling at the point of expansion for the lube oil–water case.

3.4. Pressure drop reduction factor

The key factor of viscous oil transportation is the reduction of pressure drop achieved using a less viscous fluid or water. The pressure reduction factor (Δp_r) was introduced by Russell and Charles (1959) and defined as

$$\Delta p_r = \frac{\Delta p_{ow}}{\Delta p_{so}} \quad (1)$$

where Δp_{ow} is the measured two-phase pressure drop and Δp_{so} is the pressure drop that would occur if oil flows alone in the pipeline. In this work, attempts have been made to estimate Δp_r for different flow patterns. For this, Δp_{so} has been obtained from the following equation:

$$\Delta p_{so} = \frac{32\mu_o L U_{so}}{D^2} \quad (2)$$

since the high viscosity of oil ensures laminar flow over the entire range of experimental conditions when only oil flows through the pipe. In Eq. (2) μ_o is the viscosity of the oil, U_{so} is the superficial velocity of the oil, L is the pipe length and D is the pipe diameter.

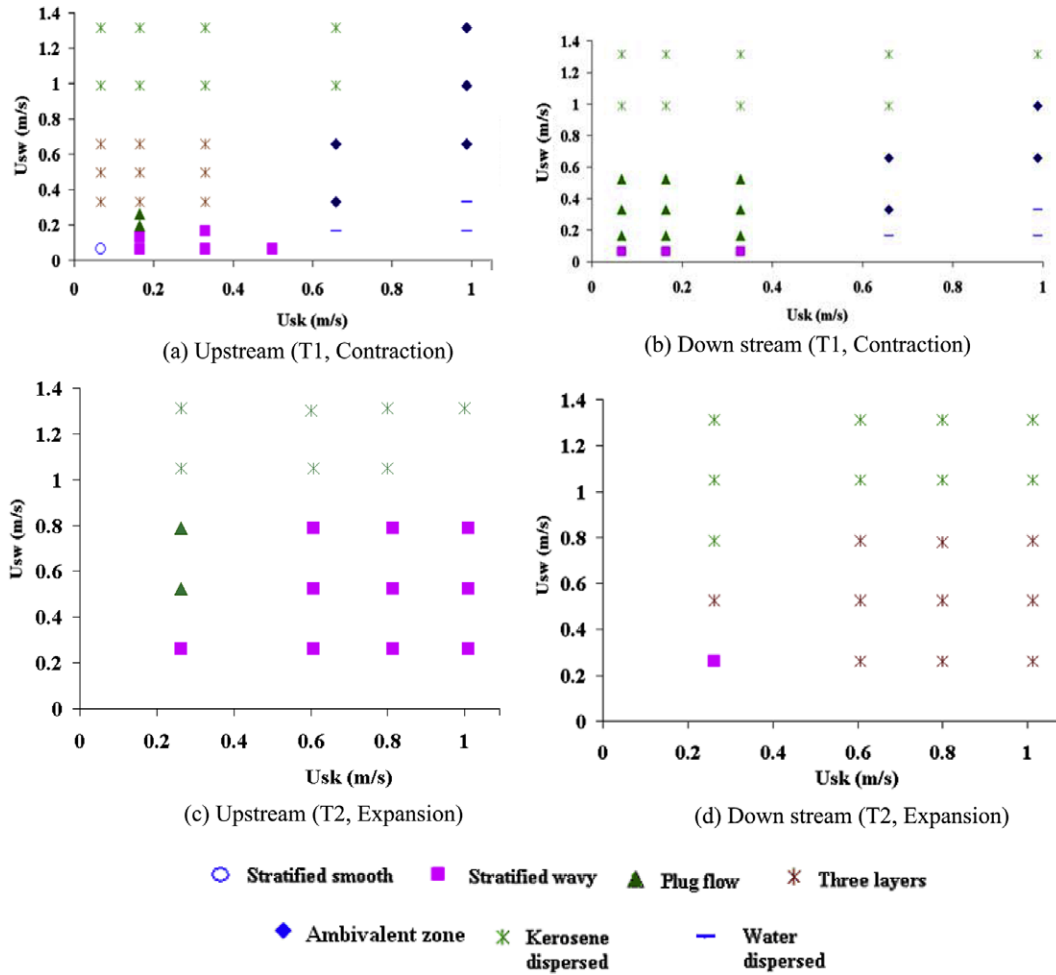


Fig. 6. Flow pattern maps for kerosene–water sudden contraction/expansion.

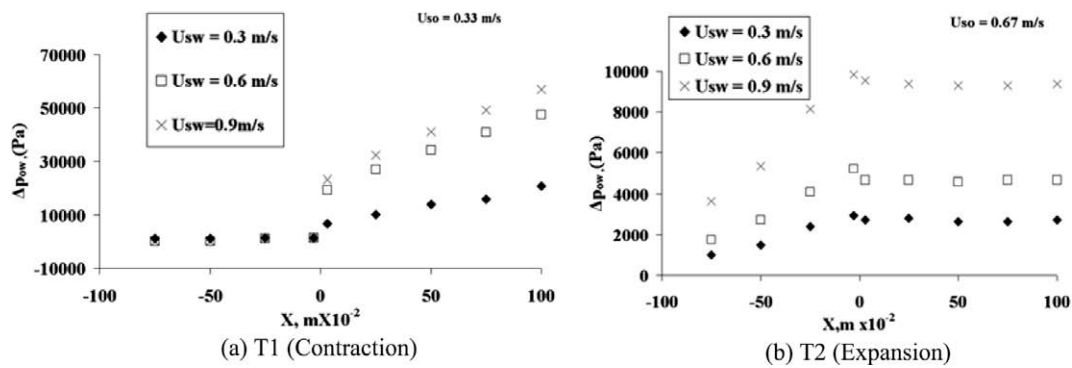


Fig. 7. Pressure profiles in sudden contraction/expansion of lube oil–water.

The typical pressure profile for contraction and expansion are shown in Fig. 9a and b, respectively. Both the figures comprise of three parts, namely part A representing the pressure profile at the upstream section, part B representing the pressure change at the plane of area change and part C for the downstream section. Since Eq. (1) is valid for straight pipes only, Δp_{ow} has been estimated experimentally from the data of parts A and C of T1 and T2. Δp_i is estimated separately for the upstream and downstream sections and presented as function of inlet water fraction (β) in Fig. 10a–d.

The inlet water fraction (β) is defined as follows:

$$\beta = \frac{Q_w}{Q_w + Q_o} \quad (3)$$

It is observed that the pressure reduction factor for core annular flow is less than that of the other flow patterns and the factor is lesser for thicker cores. The studies thus reveal that while thin core reduces the chances of pipe fouling, a thick core is preferable for lower pressure drops.

3.5. Contraction/expansion loss coefficient from experimental pressure profiles

Attempts have next been made to estimate the loss coefficients during liquid–liquid flow across contraction and expansion. The conventional approach adopted for single-phase flow is used in the present case with the estimation being based on mixture

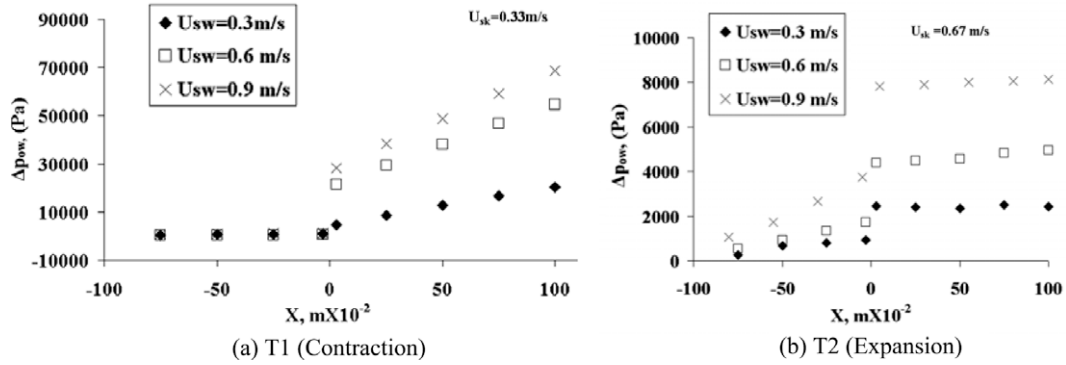


Fig. 8. Pressure profiles in sudden contraction/expansion of kerosene–water.

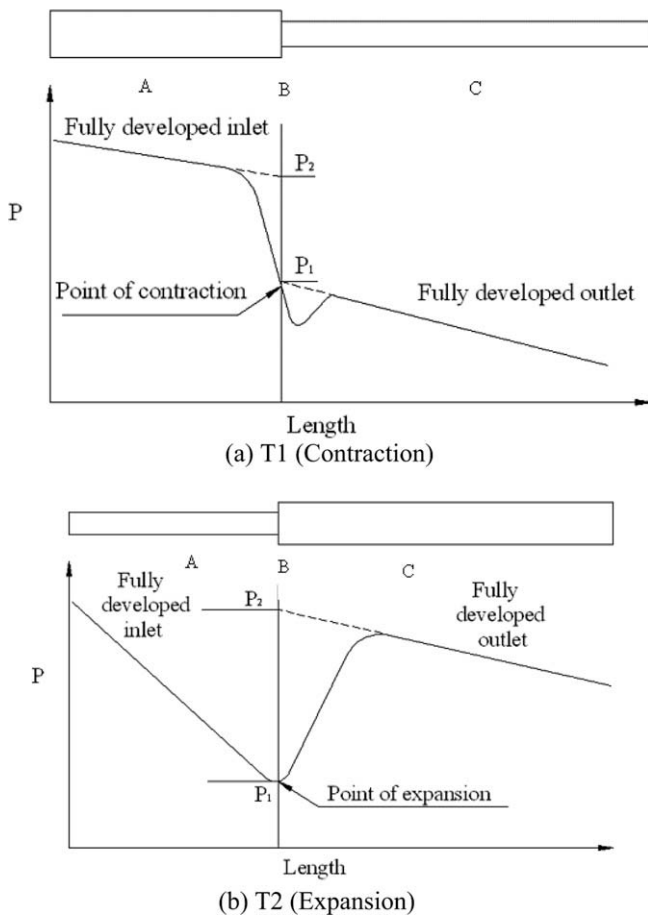


Fig. 9. Schematic of pressure variation along the flow path.

density and average velocity of the two-phase mixture in the smaller pipe.

From Bernoulli's principle at the plane of area change, we get:

$$\frac{\Delta p}{\rho_m} \pm \frac{(\sigma^4 - 1)U_m^2}{2} = h_f \quad (4)$$

where Δp is the pressure difference at the plane of area change and is obtained by extrapolating the fully developed pressure gradient profile from upstream and downstream to the point of contraction or expansion. It is measured experimentally using the data of part B in Fig. 9a and b. h_f is the frictional energy loss per unit mass and U_m

is the average mixture velocity in the smaller pipe. σ is the ratio of the diameters of the smaller and larger pipe. It is 0.5 in the present case.

ρ_m is the mixture density expressed as:

$$\rho_m = \beta\rho_w + (1 - \beta)\rho_o \quad (5)$$

Using the conventional notation

$$h_f = k_1 \frac{U_m^2}{2} \quad \text{for a contraction} \quad (6)$$

$$h_f = k_2 \frac{U_m^2}{2} \quad \text{for an expansion} \quad (7)$$

where the k_1 and k_2 denote the respective loss coefficients.

The uncertainty in estimation of k_1 and k_2 are estimated by considering the factors which influence the loss coefficients. From Eq. (4) it is noted that the values of k_1 and k_2 vary with pressure difference, mixture velocity and mixture density. Accordingly, the uncertainty in estimating k_i (δk_i) is expressed as (Holman, 1989):

$$\delta k_i = \left[\left(\frac{\partial k_i}{\partial U} \delta U_m \right)^2 + \left(\frac{\partial k_i}{\partial (\Delta p)} \delta (\Delta p) \right)^2 + \left(\frac{\partial k_i}{\partial \rho_m} \delta \rho_m \right)^2 \right]^{1/2} \quad (8)$$

where $i = 1$ for contraction and 2 for expansion. δU_m , $\delta (\Delta p)$ and $\delta \rho_m$ denote the errors in the estimation of mixture velocity, pressure and mixture density, respectively. Based on the above equation one gets a maximum uncertainty of 2.5% in estimating k_i under two-phase flow conditions. The maximum error occurs for kerosene–water flow through contraction. In case of lube oil–water, the maximum error is always estimated to be less than 1%.

Fig. 11a and b represents the respective variation of k_1 and k_2 with mixture velocity. In both the cases, the black, green and pink points refer to single-phase water, kerosene–water and lube oil–water, respectively. Interestingly, for each fluid system, a single best-fit line is observed to provide a satisfactory correlation for data in the different flow regimes. A close observation of both the figures reveal that the loss coefficients for two-phase flow is less than that obtained for only water flow through the pipeline and the loss coefficients are lower for kerosene–water as compared to lube oil–water flow.

An interest was next felt to compare the k values with the values reported in the literature. A survey of the past literature shows that several researchers have proposed empirical correlation to predict the loss coefficients for single-phase flow through contraction as well as expansion. The only work on low viscosity oil–water flow is due to Hwang and Pal (1997). Tables 2a and 2b list the relationships and the corresponding values obtained for k_1 and k_2 for the present experimental condition. From the tables it is evident that most of the researchers have expressed k as the function of

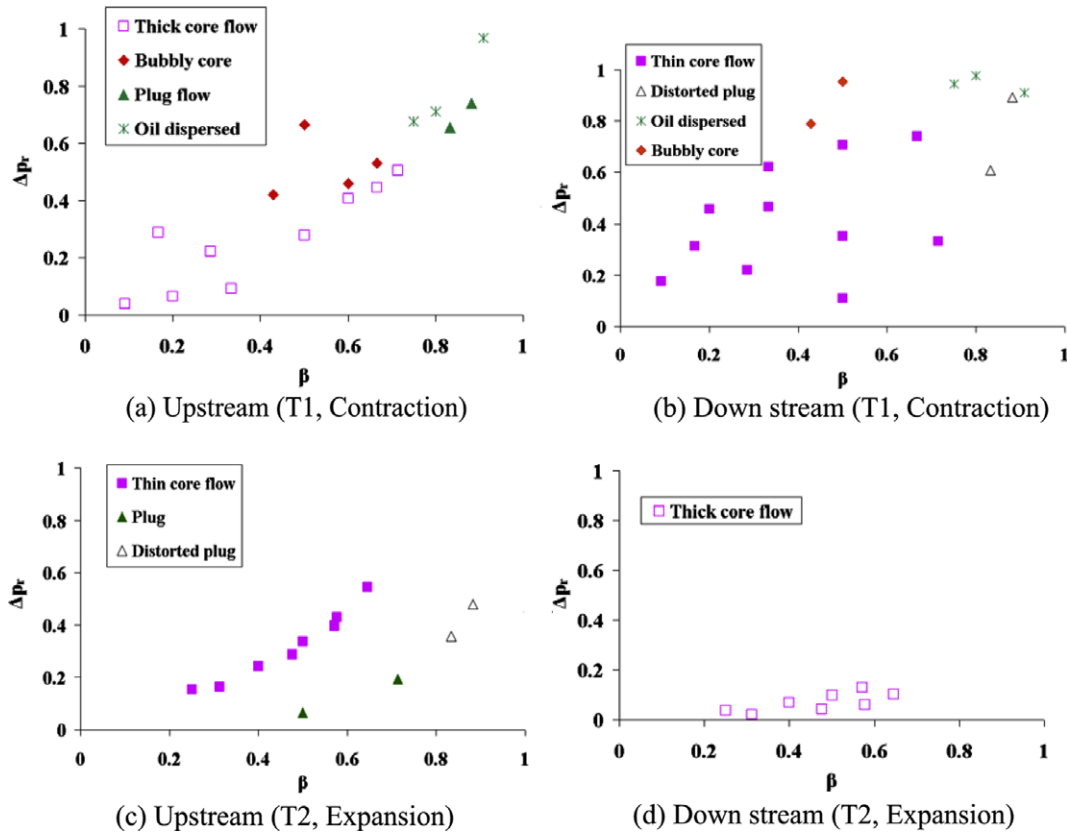


Fig. 10. Pressure reduction factor for lube oil–water in sudden contraction/expansion.

diameter ratio only and the influence of fluid properties have not been considered. Moreover, Table 2a shows that the value of k_1 varies over a wider range from 0.3 by McCabe et al. (1993) to 0.64 by Chishlom (1983). The k_1 values estimated from the present experiments for single-phase water flow is close to the value obtained from Chishlom (1983) correlation. The other relationships show consistently lower values. Further the k_1 obtained for liquid–liquid flows is lower than that reported by Hwang and Pal (1997) for oil–water emulsion. On the other hand, the k_2 values for oil–water flows in Table 2b is closer to the value reported by Hwang and Pal (1997) for flow through expansion. The experimental value of k_2 for water flow has been compared with the head loss coefficient obtained by Borda–Carnot formulation described in Massey (2001) as well as the correlation proposed by Wadle (1989). It is observed that the experimental k_2 is closer to the former value.

4. Conclusions

From the above study it can be concluded that

- An abrupt area change does influence the interfacial distribution during oil–water flow through a horizontal pipe. The influence is more pronounced for lube oil–water as compared to kerosene–water flow.
- Significant differences in flow distribution have been noted in a pipe depending on its location prior to or after the abrupt area change. Therefore, gross errors can occur in the prediction of flow patterns if the exact condition of flow is not taken into account.
- Thick core flow can be established for high viscous oil after a sudden expansion in a horizontal flow path. This can be exploited to design a suitable nozzle to ensure a wide range of stable core flow. However, this increases the chances of pipe wall fouling by the oil.
- On the other hand, a contraction in the flow passage reduces the thickness of the oil core and decreases the chances of wall fouling. This can be attributed to a reduced thickness of the oil core as well as an increase of superficial velocities.
- The flow patterns are influenced by oil properties. While viscous oils have a tendency to form different types of core annular flow, lighter oils exhibit a wider variety of distribution in water.
- Certain unique flow patterns namely sinuous core, thin core and wavy plugs have been observed during the simultaneous flow of water and highly viscous oils. Further studies are required for a thorough characterization of these flow regimes.
- The pressure profiles have been observed to be independent of oil viscosity although the formation of core flow reduces the pressure drop for viscous oils.
- The pressure reduction factor for core flow is less than that for the other flow patterns and it reduces further for thicker cores. The past studies have indicated that the optimum reduction factor for a thick core flow is a function of water cut and pipe diameter. Hence, considering requirements of pumping power, a thick core flow pattern is preferable for economic transportation.
- The experimental values of contraction and expansion coefficients are found to be lower for oil–water as compared to only water flow through the same test rigs. Further, both in case of lube oil–water as well as kerosene–water flow, the loss coefficients are observed to be independent of flow patterns.

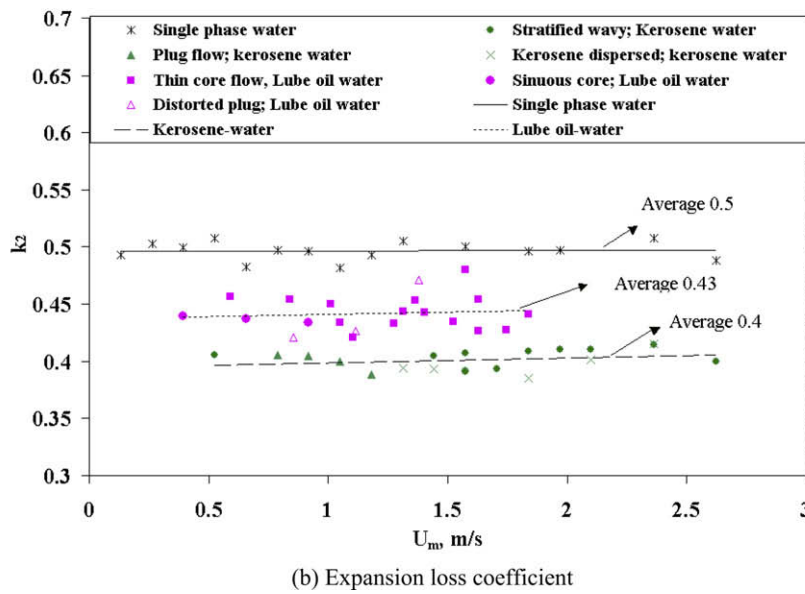
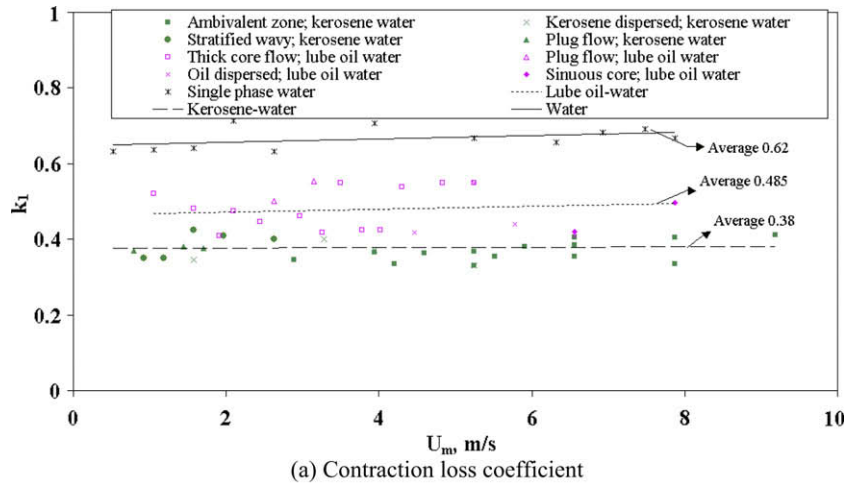


Fig. 11. Loss coefficients in sudden contraction and expansion.

Table 2a
Sudden contraction loss coefficient.

Test fluid	Estimation of k_1				
	From experiments	Reported in the literature by			
		Benedict et al. (1966)	Chishlom (1983) $k_1 = \frac{1}{[0.639(1-\sigma^2)^{0.5}+1]}$	McCabe et al. (1993) $k_1 = 0.4(1-\sigma^2)$	Hwang and Pal (1997)
Water	0.62	0.485	0.64	0.3	0.54 (for oil–water emulsion)
Kerosene–water	0.38				
Lube oil–water	0.48				

Table 2b
Sudden expansion loss coefficient.

Fluid pair	Estimation of k_2			
	From experiments	Reported in the literature by		
		Borda–Carnot equation, Massey (2001) $k_2 = (1-\sigma^2)^2$	Wadle (1989) $k_2 = 2\sigma^2(1-\sigma^2)$	Hwang and Pal (1997)
Water	0.5	0.563	0.375	0.47 (for oil–water emulsion)
Kerosene–water	0.4			
Lube oil–water	0.43			

- The close value of k_s for both the oils suggests that the loss coefficients estimated for low viscous oil–water flow can be used as a rough estimate for high viscous oil–water cases where experimentation is relatively difficult.

References

- Ahmed, W.H., Ching, C.Y., Shoukri, M., 2007. Pressure recovery of two-phase flow across sudden expansions. *Int. J. Multiphase Flow* 33, 575–594.
- Ahmed, W.H., Ching, C.Y., Shoukri, M., 2008. Development of two-phase flow downstream of a horizontal sudden expansion. *Int. J. Heat Fluid Flow* 29, 194–206.
- Angeli, P., Hewitt, G.F., 2000. Flow structure in horizontal oil–water flow. *Int. J. Multiphase Flow* 26, 1117–1140.
- Arney, M.S., Bai, R., Guevara, E., Joseph, D.D., Liu, K., 1993. Friction factor and hold up studies for lubricated pipelining – 1. Experiments and correlations. *Int. J. Multiphase Flow* 19, 1061–1067.
- Arney, M.S., Ribeiro, G.S., Bai, R., Joseph, D.D., 1996. Cement lined pipes for water-lubricated transport of heavy oil. *Int. J. Multiphase Flow* 22, 207–221.
- Bai, R., Chen, K., Joseph, D.D., 1992. Lubricated pipelining: stability of core-annular flow. Part 5. Experiments and comparison with theory. *J. Fluid Mech.* 240, 97–132.
- Bai, R., Kelkar, K., Joseph, D.D., 1996. Direct simulation of interfacial waves in a high-viscosity ratio and axisymmetric core annular flow. *J. Fluid Mech.* 327, 1–34.
- Bannwart, A.C., 1998. Wavespeed and volumetric fraction in core annular flow. *Int. J. Multiphase Flow* 24, 961–973.
- Bannwart, A.C., 2001. Modeling aspects of oil–water core-annular flows. *J. Pet. Sci. Eng.* 32, 127–143.
- Benedict, R.P., Carlucci, N.A., Swetz, S.D., 1966. Flow losses in abrupt enlargements and contractions. *Trans. ASME J. Eng. Power* 88, 73–81.
- Brauner, N., 1991. Two-phase liquid–liquid annular flow. *Int. J. Multiphase Flow* 17, 59–76.
- Chakrabarti, D.P., 2006. The hydrodynamics of liquid–liquid two-phase flow through horizontal pipeline. Ph.D. Thesis, IIT Kharagpur.
- Chakrabarti, D.P., Das, G., Ray, S., 2005. Pressure drop in liquid–liquid two-phase horizontal flow: experiment and prediction. *Chem. Eng. Technol.* 28, 1003–1009.
- Charles, M.E., Govier, G.W., Hodgson, G.W., 1961. The horizontal pipeline flow of equal density of oil–water mixtures. *Can. J. Chem. Eng.* 39, 17–36.
- Chen, I.Y., Tseng, C.Y., Lin, Y.T., Wang, C.C., 2009. Two-phase flow pressure change subject to sudden contraction in small rectangular channels. *Int. J. Multiphase Flow* 35, 297–306.
- Chishlom, D., 1983. *Two-Phase Flow in Pipelines and Heat Exchangers*. Geroge Godwin, London, pp. 175–192.
- Delhaye, J.M., 1981. Singular pressure drops. In: Bergles, A.E. (Ed.), *Two-Phase and Heat Transfer in the Power and Process Industries*. Hemisphere, Washington, DC.
- Fossa, M., Guglielmini, G., 2002. Pressure drop and void fraction profiles during horizontal flow through thin and thick orifices. *J. Exp. Therm. Fluid Sci.* 26, 513–523.
- Fossa, M., Guglielmini, G., Marchitto, A., 2006. A two-phase flow structure close to orifice contractions during horizontal intermittent flows. *Int. Commun. Heat Mass Transfer* 33, 698–708.
- Geiger, G.E., 1964. Sudden contraction losses in single and two-phase flow, Ph.D. Thesis, University of Pittsburgh, USA.
- Grassi, B., Strazza, D., Poesio, P., 2008. Experimental validation of theoretical models in two-phase high-viscosity ratio liquid–liquid flows in horizontal and slightly inclined pipes. *Int. J. Multiphase Flow* 34, 950–965.
- Guglielmini, G., Muzzio, A., Sotgia, G., 1997. The structure of two-phase flow in ducts with sudden contractions and its effects on pressure drop. In: *Invited Lecture, Proceedings of the Fourth. International Conference on Experimental Heat Transfer, Fluid Mechanics and Thermodynamics*, Brussels.
- Hickox, C.E., 1971. Instability due to viscosity and density stratification in axisymmetric pipe flow. *Phys. Fluids* 14, 251–262.
- Holman, J.P., 1989. *Experimental Methods for Engineers*. McGraw-Hill, New York.
- Hwang, C.Y.J., Pal, R., 1997. Flow of two-phase oil/water mixtures through sudden expansion and contractions. *Chem. Eng. J.* 68, 157–163.
- Jana, A.K., Das, G., Das, P.K., 2006. A novel technique to identify flow patterns during liquid–liquid upflow through a vertical pipe. *Ind. Eng. Chem. Res.* 45, 2381–2393.
- Janssen, E., 1966. Two-phase pressure losses across abrupt contraction and expansion, steam water at 600–1400 psi. In: *Proceedings of the Third International Conference on Heat Transfer*, vol. 5, New York.
- Joseph, D.D., Bai, R., Chen, K.P., Renardy, Y.Y., 1997. Core-annular flows. *Annu. Rev. Fluid Mech.* 29, 1–30.
- Mandal, T.K., Chakrabarti, D.P., Das, G., 2007. Oil water flow through different diameter pipes – similarities and differences. *Chem. Eng. Res. Des.* 85, 1–7.
- Massey, B., 2001. *Mechanics of Fluids*. Nelson Thrones Ltd., UK.
- McCabe, W.L., Smith, J.C., Harriott, P., 1993. *Unit Operations of Chemical Engineering*. McGraw-Hill, New York.
- McGee, J.W., 1966. Two-phase flow through abrupt expansions and contractions, Ph.D. Thesis, University of North Carolina, USA.
- Oliemans, R.V.A., Ooms, G., Wu, H.L., Duijvestijn, A., 1987. Core annular oil/water flow: the turbulent-lubricating – film model and measurements in a 5 cm pipe loop. *Int. J. Multiphase Flow* 13, 23–31.
- Ooms, G., Poesio, P., 2003. Stationary core-annular flow through a horizontal pipe. *Phys. Rev. E* 68, 066301–166307.
- Ooms, G., Segal, A., Vanderwee, A.J., Meerhoff, R., Oliemans, R.V.A., 1984. A theoretical model for core-annular flow of a very viscous oil core and a water annulus through a horizontal pipe. *Int. J. Multiphase Flow* 10, 41–60.
- Ooms, G., Vuijk, C., Poesio, P., 2007. Core-annular flow through a horizontal pipe: hydrodynamic counterbalancing of buoyancy force on core. *Phys. Fluids* 19, 092103.
- Parida, V.J.W., Bannwart, A.C., 2001. Modeling of vertical core-annular flows and application to heavy oil production. *J. Energy Resour. Technol.* ASME 123, 194–199.
- Preziosi, L., Chen, K., Joseph, D.D., 1989. Lubricated pipelining: stability of core-annular flow. *J. Fluid Mech.* 201, 323–356.
- Rodriguez, O.M.H., Bannwart, A.C., 2006. Analytical model for interfacial waves in vertical core flow. *J. Pet. Sci. Eng.* 54, 173–182.
- Russell, T.W.F., Charles, M.E., 1959. The effect of less viscous liquid in the laminar flow of two immiscible liquids. *Can. J. Chem. Eng.* 37, 18–24.
- Santos, R.G., Mohamed, R.S., Bannwart, A.C., Loh, W., 2006. Contact angle measurements and wetting behavior of inner surfaces of pipelines exposed to heavy crude oil and water. *J. Pet. Sci. Eng.* 51, 9–16.
- Schmidt, J., Friedel, L., 1997. Two-phase pressure drop across sudden contraction in duct areas. *Int. J. Multiphase Flow* 23, 283–299.
- Silva, R.C.R., Mohamed, R.S., Bannwart, A.C., 2006. Wettability alteration of internal surfaces of pipelines for use in the transportation of heavy crude oil via core flow. *J. Pet. Sci. Eng.* 51, 17–25.
- Sotgia, G., Tartarini, P., Stalio, E., 2008. Experimental analysis of flow regimes and pressure drop reduction in oil–water mixtures. *Int. J. Multiphase Flow* 34, 1161–1174.
- Taitel, Y., Dukler, A.E., 1976. A model for predicting flow regime transitions in horizontal and near horizontal gas–liquid flow. *Am. Inst. Chem. Eng. J.* 22, 47–55.
- Wadle, M., 1989. A new formula for the pressure recovery in an abrupt diffuser. *Chem. Eng. J.* 15, 241–256.